

# Thermodynamic Features of Myosin Filament Suspensions: Implications for the Modeling of Muscle Contraction

Enrico Grazi and Orietta Cintio

Dipartimento di Biochimica e Biologia Molecolare, Università di Ferrara, 44100 Ferrara, Italy

**ABSTRACT** The analysis of myosin filament suspensions shows that these solutions are characterized by highly nonideal behavior. From these data a model is constructed that allows us to predict that 1) when subjected to an increasing protein osmotic pressure, myosin filaments experience an elastic deformation, which is not linearly related to the acting force; and 2) at constant protein osmotic pressure, when the cross-bridges of the myosin filaments are subjected to an external, nonosmotic force parallel to the filament axis, they are deformed and the water activity coefficient is altered. As a consequence, in muscle, passive and active shortening of the sarcomere is expected to promote the change of the water-water and of the water-protein interactions. We thus propose to depict muscle contraction as a chemo-osmoelastic transduction, where the analysis of the energy partition during the power stroke requires consideration of the osmotic factor in addition to the chemoelastic ones.

## INTRODUCTION

For a few years we have studied the osmotic properties of the proteins of the contractile system: F-actin (Grazi et al., 1993, Schwenbacher et al., 1995), the myosin subfragment-1 (Grazi et al., 1995), the myosin subfragment S1-F-actin complex (Grazi et al., 1994), and the actomyosin complexes (Magri et al., 1996). From these studies the concept originated that protein osmotic pressure influences both the shape and the elastic properties of these hydrated proteins. Accordingly, both the diameter and the intermonomer contacts of the actin filament were proposed to change with protein osmotic pressure (Grazi, 1997) and the stiffness of the attached cross-bridge was proposed to depend on the protein osmotic pressure, generated by the components of the attached cross-bridge itself (Grazi et al., 1996a, b). These phenomena are better understood when the model dismisses the contractile structure as an assembly of “solid” bodies and the model accepts the contractile structure as an ordered, highly nonideal solution. The solution is ordered because of the protein-protein recognition and is highly nonideal because of the high concentration (mmolal order) of its protein components. A fairly adequate representation of the contractile apparatus can thus be based on both thermodynamic (nonideality) and geometric (protein-protein recognition) considerations, with the important corollary that protein-protein recognition and nonideality are interconnected, so that at any time the interaction of two proteins changes the nonideality of the system, and vice versa.

A good example of this situation is provided by the high nonideality of the myosin filaments and by their behavior

under the effect of osmotic and mechanic external forces. Our observations point to a direct connection between the action of a mechanic force and the state of the solvent, and suggest that in muscle, passive and active shortening of the sarcomere promote the change of the water-water and of the water-protein interactions. It is therefore proposed that muscle contraction has to be described as a chemo-osmoelastic transduction, where the analysis of the energy partition during the power stroke requires consideration of the osmotic factor in addition to the chemoelastic ones.

## MATERIALS AND METHODS

Myosin and myosin rods were prepared from rabbit muscle (Margossian and Lowey, 1982). Molar concentration of myosin was calculated on the basis of the molecular mass of 470 kDa, and the absorption coefficient used was  $A_{280}^{1\%}$  of 5.3 (Margossian and Lowey, 1982). Molar concentration of myosin rods was calculated on the basis of the molecular mass of 220 kDa and the absorption coefficient used was  $A_{280}^{1\%}$  of 2.2.

Bipolar myosin filaments were prepared according to Honda and Asakura (1989). In our hands this procedure gave rise to filaments of the average length of  $\sim 0.8 \mu\text{m}$ .

Buffer solutions for osmotic stress experiments contained (in 1000 g of water): KCl, 0.1 mol; triethanolamine, 0.01 mol;  $\text{MgCl}_2$ ,  $\text{NaN}_3$ , 2-mercaptoethanol 2 mmol each. pH was taken to 7.5 with 6 M HCl.

Solutions of either myosin filaments or the rods were prepared and dialysed for 17 h at  $2^\circ\text{C}$  against the above buffer. The osmotic pressure of the protein system was measured using a secondary osmometer: protein solutions (1 ml) were equilibrated by dialysis against buffer solutions (100 ml) supplemented with weighed amounts of poly(ethyleneglycol) 40,000. The osmotic pressure associated with the poly(ethyleneglycol) solutions was measured directly with a pressure gauge (Schwenbacher et al., 1995). Equilibration of protein solutions was carried out for 48–96 h at  $22^\circ\text{C}$  in stopped bottles, immersed in a shaking water bath thermostatically controlled to within  $\pm 0.1^\circ\text{C}$ . At the end of the equilibration protein concentration was measured as previously described (Schwenbacher et al., 1995; Magri et al., 1996).

For electron microscope observation, bipolar myosin filaments were diluted with the same suspension buffer to a protein content of 0.1 mg/ml and immediately applied to carbon-coated 400 mesh grids, washed once with a drop of water, and stained with five drops of 1% uranyl acetate, pH 4.25.

Received for publication 25 July 2000 and in final form 16 April 2001.

Address reprint requests to Dr. Enrico Grazi, Dipartimento di Biochimica e Biologia Molecolare, Università di Ferrara, via Borsari 46, 44100 Ferrara, Italy. Tel.: 39-0532-291421; Fax: 39-0532-202723; E-mail: gre@ifeuniv.unife.it.

© 2001 by the Biophysical Society

0006-3495/01/07/313/08 \$2.00

## RESULTS

### Myosin filament suspensions are highly nonideal solutions

Myosin filament suspensions are equilibrated by dialysis against poly(ethyleneglycol) 40,000 solutions of known macromolecular osmotic pressure. At the equilibrium, when the protein osmotic pressure of the sample is the same as the macromolecular osmotic pressure of the poly(ethyleneglycol) solutions, the molality of myosin is determined. In Fig. 1 the protein osmotic pressure,  $\pi$ , associated with the samples is plotted against the molality of myosin (as monomer),  $m$ .

The behaviour diverges significantly from that predicted for an ideal solution:

$$\pi = -RT \ln[X_w](\text{Pa}),$$

or, in the molal scale:

$$\pi \sim m_m RT(M_w/V_w) = 1000 m_m RT(\text{Pa}),$$

where  $X_w$  is the water molar fraction;  $M_w = 0.018 \text{ kg}$  is the water molal mass;  $V_w = 18 \times 10^{-6} \text{ m}^3$  is the water partial molal volume.

The data are described by the expression:

$$\pi = 10^3 RT(m + 1.7 \times 10^{10} m^4) \quad (1)$$

Thus the filament solutions are highly nonideal.

### The chemical potential of myosin as a function of protein osmotic pressure

As a first approximation, the chemical potential of the diffusible species but water is considered not to change significantly in the course of the experiment. In fact, measured protein osmotic pressure does not change significantly when ionic strength is changed between 0.1 and 0.15 M. As

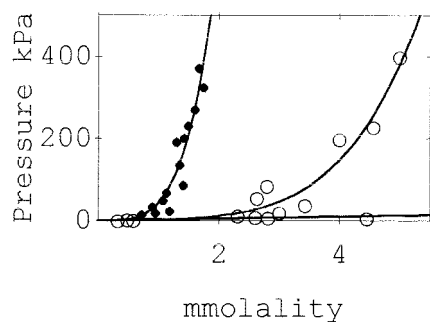


FIGURE 1 Protein osmotic pressure as a function of the molality of myosin. Concentration, mmolality; pressure, kPa. Myosin (filled circles): data are fitted by the curve  $\pi = 10^3 RT(m + 1.7 \times 10^{10} m^4)$  (Pa against molality). Myosin rods (open circles): data are fitted by the curve  $\pi = 1000 RT(m_r + 2 \times 10^9 m_r^4)$ . The pressure generated by an ideal solution,  $\pi = 10^3 RT m$ , in this scale almost coincides with the bottom line of the figure.

a consequence, the system can be considered as a binary system composed of water and myosin.

By making use of the Gibbs-Duhem relation:

$$n_w d\mu_w + n_m d\mu_m = 0 \quad (2)$$

where  $d\mu_m$  and  $d\mu_w$  are the chemical potential changes of myosin and water, and  $n_m$  and  $n_w$  are the number of moles of myosin and water, respectively; the change of the chemical potential of myosin as a function of myosin molality is calculated:

$$\begin{aligned} d\mu_m &= -n_w/n_m d\mu_w; \\ d\mu_m &= -55.5555/md\mu_w \end{aligned} \quad (3)$$

since

$$\mu_w = \mu_w^\circ + RT \ln[a_w] \quad \text{and} \quad \pi \times V_M = -RT \times \ln[a_w],$$

$d\mu_w = -V_M d\pi$  and Eq. 3 becomes:

$$d\mu_m = 55.5555/mV_M d\pi \quad (4)$$

where  $V_M = 18 \times 10^{-6} \text{ m}^3$  is the water partial molar volume,  $\pi$  is the protein osmotic pressure, and  $a_w$  is the activity of water.

Since

$$\begin{aligned} \pi &= 10^3 RT(m + 1.7 \times 10^{10} m^4) \\ &= \frac{RT(m + 1.7 \times 10^{10} \times m^4)}{V_M \times 55.5555} \end{aligned} \quad (\text{Eq.1})$$

$d\pi$  can be expressed as

$$d\pi = \frac{d \frac{RT(m + 1.7 \times 10^{10} \times m^4)}{V_M \times 55.5555}}{dm} \times dm \quad (5)$$

By introducing the new expression for  $d\pi$  into Eq. 4 we obtain:

$$\begin{aligned} d\mu_m &= 55.5555/mV_M \\ &\times \frac{d \frac{RT(m + 1.7 \times 10^{10} \times m^4)}{V_M \times 55.5555}}{dm} \times dm \end{aligned} \quad (6)$$

$\mu_m$  is obtained by integration of Eq. 6:

$$\mu_m = RT(2.26666 \times 10^{10} m^3 + \ln[m]) + \text{const} \quad (7)$$

In the calculation of  $\Delta\mu$  the integration constant cancels out (Fig. 2).

### The model

The data presented on the thermodynamic properties of the myosin filament solutions allow building a model relating

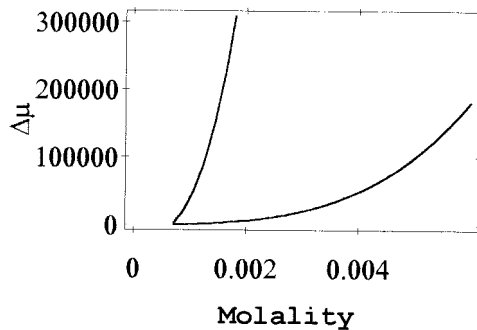


FIGURE 2 Chemical potential change of myosin as a function of myosin molality. Concentration, molality;  $\Delta\mu$ , Joules/mol. The  $\Delta\mu$  of myosin (*left curve*) was calculated by making use of the equation  $\mu_m = RT(2.26666 \times 10^{10} m^3 + \ln[m]) + \text{cost}$  (see Eq. 7). The molality of reference was  $0.72 \times 10^{-3}$  molal. The  $\Delta\mu$  of the myosin rods (*right curve*) was calculated by making use of the equation  $\mu_r = RT(2.58823 \times 10^9 m_r^{3.4} + \ln[m_r])$  (see Eq. 21). The molality of reference was  $0.72 \times 10^{-3}$  molal.

osmotic phenomena (water chemical potential changes) to elastic phenomena (protein chemical potential changes and external work applied to the cross-bridge). To achieve this goal we recognize first that, beyond a given myosin concentration (or a given protein osmotic pressure), any change of the volume of the solution is accompanied by a change of the volume of the hydrated filament, thus of the radius of the hydrated filament. This allows us to set a relationship between the molality of myosin and the radius of the hydrated filament. Second, we set the equivalence between pressure-volume work and elastic stress, we assume that the stress is mostly localized to the cross-bridges, and calculate the dependence of cross-bridge distortion on myosin concentration (or protein osmotic pressure). Third, we calculate the “force length constant” and show that, according to our model, it increases significantly with cross-bridge distortion. Fourth, we show that, at constant protein osmotic pressure, applying an external force to cross-bridges decreases the activity coefficient of water. This means that, according to our model, the nonosmotic force  $F_{\text{EX}}$  influences both cross-bridge deformation and water-water and water-myosin interactions.

### The volume of the solution and the geometric constraints

The volume of the solution (with reference to one mole of myosin) is:

$$V = 10^{-3}m^{-1} + pmv(m^3) \quad (8)$$

where  $m$  is the molality of myosin, and  $pmv = 0.34216 \text{ m}^3$  is the partial molar volume of myosin, obtained by multiplying the molar mass of myosin (470 kDa) (Margossian and Lowey, 1982) by its partial specific volume  $0.728 \text{ cm}^3 \text{ g}^{-1}$  (Kielley and Harrington, 1960).

By increasing macromolecular osmotic pressure, water is withdrawn and the volume of the solution decreases. Above a given pressure most of the volume of the solution is occupied by filaments, which are forced to stack, their lengths paralleling each other. The orthogonal section of these stacks is approximately represented in Fig. 3, where the segment AB is the interfilament distance or the diameter of the filaments. Simple trigonometric considerations relate the volume of the solution to the diameter of the filaments as follows:

$$V = N/n \times 2\sqrt{3} \times r^2 \times le \quad (9)$$

Where  $N$  is the Avogadro number and  $n$  is the number of molecules of myosin per filament; thus,  $N/n$  is the number of filaments per mol of myosin,  $le$  is the length of the filament, and  $2\sqrt{3}r^2$  is the section of the elementary unit involving both the intra and the extrafilament spaces (Fig. 3). When the volume of the solution approaches the volume of the filaments, by equating expressions (8) and (9), the average radius of the hydrated filaments can be determined provided that the average length of the filaments and the average number of molecules of myosin per filament is known:

$$r = \sqrt{\frac{n \times (10^{-3} \times m^{-1} + pmv)}{2\sqrt{3} \times le \times N}} (m) \quad (10)$$

In rabbit psoas sarcomere the thick filament has a length of  $1.57 \mu\text{m}$  (Craig and Hoffer, 1976; Sjoström and Squire, 1977), shaft and cross-bridge diameter of 15 nm and 30.1 nm (Ip and Heuser, 1983), and is composed of  $\sim 400$  myosin molecules. Our myosin filaments, prepared by the procedure of Honda and Asakura (1989), display an average length of  $\sim 0.8 \mu\text{m}$  and are assumed to be composed of  $\sim 200$  myosin molecules. Thus they are a good model to study the osmotic properties of the thick filament.

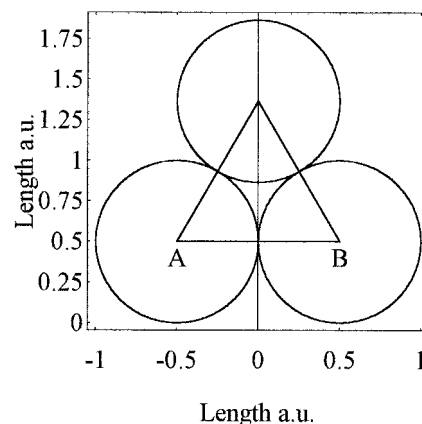


FIGURE 3 Orthogonal section of the stacks of myosin filaments. AB is the average interfilament distance.

### Equivalence between the pressure-volume work and the elastic stress

While the volume of the solution decreases, the myosin filaments are elastically stressed. We assume that the stress is mostly localized to the cross-bridges, so that cross-bridge distortion,  $x$ , is tightly coupled to cross-bridge rotation. A schematic representation of the phenomenon is given in Fig. 4. The segment  $CC'$  represents the axis of the half-filament, where  $C'$  is the end of the filament and  $C$  is the middle of the filament. The segment  $OA$  represents the cross-bridge at zero elastic stress (angle  $\alpha = AOC$ ) and zero distortion. The segment  $OB$  represents the cross-bridge at a given elastic stress (angle  $\alpha = BOC$ ) and at the distortion,  $x = OD = OB \cos \alpha$ .

In this model the radius of the filament decreases from  $r_0 = AO$ , at zero elastic stress, to  $r = BD = OB \sin \alpha$  at a given elastic stress. Thus,

$$\sin \alpha = \frac{r}{r_0} \quad (11)$$

The model allows us to calculate the elastic force,  $F$ , directed toward the center of the filament and acting on each single molecule of myosin:

$$F = \frac{\pi}{N} \times \frac{dV}{dr} \quad (12)$$

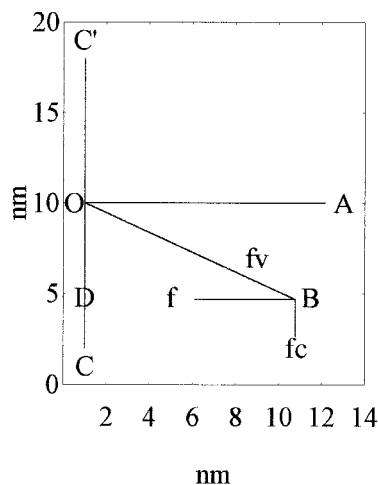


FIGURE 4 Cross-bridge orientation in one half of the myosin filament.  $CC'$  is the axis of the myosin filament, where  $C'$  is toward the end of the filament and  $C$  is toward the middle of the filament.  $r_0 = OA$  and  $AOC = 90^\circ$  are the radius of the myosin filament and the angle  $\alpha$  at protein osmotic pressure  $\sim 0$ ;  $r = BD = BO \sin(\alpha)$  and  $BOC$  are the radius of the myosin filament and the angle  $\alpha$  at the experimental protein osmotic pressure;  $F$  is the force orthogonal to the filament axis, acting on each cross-bridge;  $F_v$  is the component directed toward the constraint;  $F_c$  is the component parallel to the filament axis and directed toward the center of the filament.

where

$$\frac{dV}{dr} = \frac{N}{n} \times le \times 4\sqrt{3} \times r \quad (13)$$

From the force  $F$  the force  $F_c$ , parallel to the axis and directed toward the center of the filament, and the distortion,  $x$ , are calculated:

$$F_c = \pi \times \frac{4}{n} \times \sqrt{3} \times le \times r \times \frac{\cos(\alpha)}{\sin(\alpha)} \quad (14)$$

or the equivalent expression

$$F_c = \pi \times \frac{4}{n} \times \sqrt{3} \times le \times \sqrt{r_0^2 - r^2} \quad (14a)$$

$$x = r_0 \times \cos(\alpha) \quad (15)$$

In fact, two different models of the thick filaments are used.

The first and simpler model assumes that the rotating portion equals  $r_0$ . In this case  $r = r_0 \times \sin(\alpha)$ . The second model assumes that the length of the rotating portion is half of the difference between the cross-bridge diameter, 30.1 nm, and the shaft diameter, 15 nm, thus equals 7.55 nm. In this case  $\sin(\alpha) = (r - b)/(r_0 - b)$ , where  $b = r_0 - 7.55$  nm.

The calculations (Table 1) are performed at myosin concentrations between 0.7 and 1.7 mmolal, which correspond to the protein osmotic pressures of 11.7 kPa and 352 kPa, respectively. In this range of concentrations myosin filaments stack to each other. As shown in Table 1, the length of the rotating arm (15.05 nm first model and 7.5 nm second model), has a large influence on the value of the angle  $\alpha$ . At the myosin concentration of 1.7 mmolal the value of the angle  $\alpha$  is  $44.4^\circ$  for the first model and  $23.7^\circ$  for the second model.

### The “force length constant” and protein osmotic pressure

Analysis of the osmotic properties of myosin by means of models I and II allows us to estimate the “force length constant,”  $k = F_c/x$ , for the distortion of the cross-bridges.

TABLE 1 The elastic compression in two models of the myosin filament

	Mmolality	Radius (nm)	Angle alpha	$F_c$ (pN)	Distortion (nm)
Model I	0.7	14.55	75.2	1.25	3.84
Model I	1.7	10.53	44.4	104.8	10.74
Model II	0.7	14.55	69.0	1.8	2.70
Model II	1.7	10.53	23.7	234.0	6.91

The length of the rotating arm is 15.05 nm in the first model and 7.5 nm in the second model. The molalities of  $7 \times 10^{-4}$  and  $1.7 \times 10^{-4}$  correspond to the protein osmotic pressures of 11.7 kPa and 352 kPa, respectively.

It is found that the “force length constant” increases significantly with the distortion,  $x$ , and that the increase depends on the length of the rotating arm (Fig. 5). By increasing protein osmotic pressure from 18 kPa to 50 kPa, the likely range of protein osmotic pressure in muscle,  $k$ , increases from 0.5 to 1.39 pN · nm<sup>-1</sup> for model I (rotating arm 15.05 nm) and from 0.79 to 3.48 pN · nm<sup>-1</sup> for model II (rotating arm 7.5 nm).

### Applying an external, nonosmotic force to the cross-bridges

Let us consider, as an example, a myosin filament suspension (0.95 mm as myosin), in equilibrium with the external macromolecular osmotic pressure of 36.25 kPa (Eq. 1), imposed by the large external reservoir. The average hydrated radius of the filaments is  $1.2909 \times 10^{-8}$  m (Eq. 10), the angle  $\alpha$  is 59.06° (Eq. 11). The force applied to each single cross-bridge is  $F_C = 7.773$  pN (Eq. 14) which, because of the action-reaction principle, is equilibrated by the elastic force due to the elastic reaction of the cross-bridge.

Let us now simulate that an external, nonosmotic force,  $F_{EX} = 0.8$  pN, with the same direction but inverse to  $F_C$  (Fig. 4) is applied to any single cross-bridge of the myosin filaments, while protein osmotic pressure is kept constant at the value of 36.25 kPa. The operation is analogous to stretching a sarcomere in rigor, with the difference that in the sarcomere attached cross-bridges are stretched, while in our case, there are stretched, unattached cross-bridges. As a result of the application of the force,  $F_{EX}$ , the equilibrium is displaced toward a lower distortion of the cross-bridges, i.e., a large radius and a larger angle  $\alpha$ . Furthermore, since the volume of the solution and cross-bridge distortion are cou-

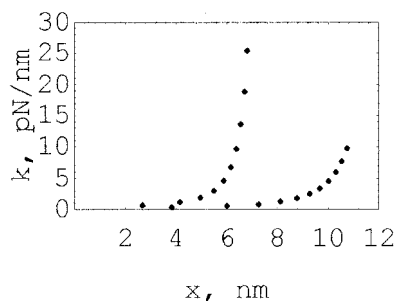


FIGURE 5 The “force length constant” as a function of the distortion. “Force length constant,”  $k = F_C/x$ . Lower trace, first model; upper trace, second model. For the first model the values of  $k$  were calculated by dividing the value of  $F_C$ , (Eq. 14a) at a given molality by the value of  $x$  (Eq. 15) at the same molality and plotting this ratio against  $x$ . The operation was then repeated for all the remaining points of the figure. The same operations were repeated for the second model except that the expressions for  $\alpha$  and  $x$  were:  $\alpha = \arcsin[(r - b)/(r_0 - b)]$  and  $x = (r_0 - b) \cos[\alpha]$ , where  $b = 7.5$  nm is half of the difference between the cross-bridge diameter and the shaft diameter.

pled (Eq. 12), water is taken up by the sample and the molality of myosin decreases.

In the new osmoelastic equilibrium the osmotic force,  $F'_C$ , equals the elastic reaction  $E'_R$  plus the force,  $F_{EX}$ , so that:

$$F'_C = E'_R + F_{EX} \quad (16)$$

$F'_C$ , for  $\pi = 36.25$  kPa, can be expressed as a function of the molality of myosin,  $m$ , by introducing expression 10, for  $r$ , into expression 14a:

$$F'_C = \pi \times \frac{4}{n} \times le \times \sqrt{3} \times \sqrt{r_0^2 - \frac{n \times (10^{-3} \times m^{-1} + pmv)}{2 \times \sqrt{3} \times le \times N}} \quad (17)$$

Similarly, the substitution of Eq. 1,  $10^3 RT(m + 1.7 \times 10^{10} m^4)$ , for  $\pi$  in Eq. 17, allows us to express  $E'_R$  as a function of the molality of myosin:

$$E'_R = 10^3 RT(m + 1.7 \times 10^{10} m^4) \times \frac{4}{n} \times le \times \sqrt{3} \times \sqrt{r_0^2 - \frac{n \times (10^{-3} \times m^{-1} + pmv)}{2 \times \sqrt{3} \times le \times N}} \quad (18)$$

At  $\pi = 36250$  Pa,  $n = 200$ ,  $le = 0.8 \times 10^{-6}$  m,  $r_0 = 15.05 \times 10^{-9}$  m,  $pmv = 0.34216$  m<sup>3</sup>, Eq. 16 is solved for  $m = 9.222 \times 10^{-4}$  molal myosin. By making use of Eqs. 8, 10, 11, 17, and 18, the volume of the solution, the hydrated radius of the filaments, the angle  $\alpha$ ,  $F'_C$ , and  $E'_R$ , respectively, are then calculated (Table 2).

A comment on Eqs. 17 and 18 is worthwhile at this stage. In Eq. 17  $\pi = 36250$  Pa is the actual protein osmotic pressure imposed on the system and dictates the value of  $F'_C$ . In Eq. 18, for  $m = 9.222 \times 10^{-4}$  molal myosin,  $10^3 RT(m + 1.7 \times 10^{10} m^4)$  is the protein osmotic pressure that would be generated in the absence of the external, nonosmotic force,  $F_{EX}$ . Equation 18 thus gives the  $F_C$  at  $m = 9.222 \times 10^{-4}$  molal myosin when  $F_{EX} = 0$ , thus the  $F_C$  is balanced by the  $E_R$ .

The displacement of the equilibrium by force  $F_{EX}$  increases the water molar fraction, mol of water/(mol of myosin + mol of water), from  $X_W = 55.5555/(55.5555 + 0.00095) = 0.9999829003$  to  $X'_W = 55.5555/(55.5555 + 0.000922) = 0.9999833989$ .

TABLE 2 Applying an external, nonosmotic force to the cross-bridge of the myosin filament

External Force (0.8 pN)	Myosin mm	$r$ (nm)	Angle alpha	Volume (l)	$F_C$ (pN)	$E_R$ (pN)
Not Applied	0.95	12.91	59.06	1390	7.773	-7.773
Applied	0.922298	13.055	60.16	1421	7.523	-6.723

The system is equilibrated at the protein osmotic pressure of 36.25 kPa. The external force applied,  $F_{EX} = 0.8$  pN, is parallel and inverse to  $F_C$ .



Because protein osmotic pressure remains constant at 36.25 kPa, water chemical potential also remains constant, thus the following relation holds:

$$\frac{\gamma_w}{\gamma'_w} = \frac{X'_w}{X_w} = 1.000000499 \quad (19)$$

where  $\gamma_w$  and  $\gamma'_w$  are the water activity coefficients before and after the application of  $F_{EX}$ . Thus force  $F_{EX}$  decreases the activity coefficient of water in the myosin filament suspension. This means that the nonosmotic force  $F_{EX}$  influences both cross-bridge deformation and water-water and water-myosin interactions.

The significance of this change of the water activity coefficient can be appreciated by considering that, by differential osmometry, protein osmotic pressure can be controlled to within 9.8 Pa (the pressure of a 1-mm water column). According to Eq. 1 a pressure increase of 9.8 Pa is given by the increase of myosin from 0.95 mm to 0.950068 mm, which corresponds to the decrease of the water molar fraction from  $X_A = 0.9999829003$  to  $X_B = 0.9999828991$ . The corresponding water activities (in the molar fraction scale),  $a$ , are calculated by the equation  $a = \exp[-\pi V_M/RT]$ , where  $\pi$  is given by Eq. 1 and  $V_M$  is the partial molar volume of water, and are, respectively,  $a_A = 0.9997336964$  and  $a_B = 0.9997336237$ . By dividing the activities by the respective molar fractions, the water activity coefficients  $\gamma_A$  and  $\gamma_B$  are obtained:  $\gamma_A/\gamma_B = 1.000000072$ . This is the lowest water activity coefficient ratio that can be appreciated in our experiments and is significantly lower than that (1.000000499) generated by applying the external force to the cross-bridge.

### Osmotic properties of the myosin rod

Like myosin solutions, rod solutions also display a nonideal behavior. Data are presented in Fig. 1 and are reasonably well described by the equation

$$\pi = 1000RT(m_r + 2 \times 10^9 m_r^{4.4}), \text{ Pa} \quad (20)$$

where  $m_r$  is the molality of the rods.

The chemical potential of the rods ( $\mu_r$ ) (Fig. 2) is calculated from osmotic pressure data by making use of a procedure identical to that followed for the myosin filaments. It is related to molality by the expression:

$$\mu_r = RT(2.58823 \times 10^9 m_r^{3.4} + \ln[m_r]) + \text{cost}, \text{ J} \cdot \text{mol}^{-1} \quad (21)$$

Owing to the large difference of the molecular masses of myosin (470 kDa) and of the rod (220 kDa), osmotic effects are best compared on an osmotic pressure basis than on a molal basis. That is to say that a comparison has to be made between the concentrations of the two structures that produce the same protein osmotic pressure. As an example, we calculate how much the concentration of the two structures

must increase to produce the same increase, let us say from 18.5 to 22 kPa, of the protein osmotic pressure. By making use of Eqs. 1 and 20, we find out that 1) myosin concentration must increase from 1.44498 mm (679 g of protein per 1000 g of water) to 1.51 mm (679 g of protein per 957 g of water), 43 cm<sup>3</sup> of water are thus withdrawn; and 2) rod concentration must increase from 4.222 mm (928.84 g of protein per 1000 g of water) to 4.3721 mm (928.84 g of protein per 960 g of water), 40 cm<sup>3</sup> of water are thus withdrawn.

The question is, will the rod mass, in myosin, behave as the average myosin mass or will it behave as the mass of the isolated rods? The question cannot be answered on the sole osmotic data.

## DISCUSSION

### Primary and secondary osmometry

Our experiments were performed by secondary osmometry, i.e., by equilibrating, through a dialysis membrane, the myosin filament suspensions against a large reservoir containing solutions of poly(ethyleneglycol) 40,000 of known macromolecular osmotic pressures. By making use of this device only the macromolecular component of the osmotic pressure is appreciated because water and small solutes diffuse freely through the dialysis membrane. The system is equivalent to primary osmometry, where a dialysis membrane separates a large reservoir of water and small solutes from the myosin filament suspension, to which a suitable hydrostatic pressure is applied to counteract water influx. By making use of these tools an endless sequence of equilibria can be experienced, where macromolecular osmotic pressure is linked to the change of the chemical potential change of the macromolecular solute, to its hydration and, by means of either model I or II, to force,  $F_C$  (Eqs. 14 and 14a) and to distortion,  $x$  (Eq. 15).

### On the origin of the elastic distortion of the cross-bridges

Beyond a given protein osmotic because of water withdrawal and of the consequent decrease of the volume of the solution, myosin filaments become closer and closer. The question is now whether distortion arises because of "crowding" or because of dehydration. There is no way to experience distortion in the absence of "crowding" because macromolecular osmotic pressure is generated by the protein itself. It is a fact, however, that the increase of protein osmotic pressure perturbs the solvent-protein interactions, thus protein hydration. No doubt that these events displace conformational equilibria and stabilize "distorted" conformations. This means that the increase of protein osmotic pressure displays a distorting effect per se.

### The “force length constant”

In the modeling of muscle contraction, the force,  $F$ , exerted by the cross-bridge along the direction of the filament, is considered to be a function only of the position of the base of the cross-bridge relative to the position of its current site of attachment. These relative positions are measured by the variable,  $x$ , referred to as the “distortion” of the cross-bridge and defined so that  $F(0) = 0$ .  $F(x)$  is usually taken as a linear function containing a force constant,  $k$ :  $F(x) = kx$  (Brokaw, 1976).

The analysis of our model indicates that force,  $F$ , is not at all a linear function of the deformation,  $x$ , and that the “length-force constant” changes significantly with the deformation as well as with the length of the rotating arm. Attached cross-bridges are thus expected to behave similarly in muscle.

### Cross-bridge deformation and water structure

From the analysis of our model it appears that elastic deformation of the cross-bridge and water structure are coupled. Coupling occurs not only when cross-bridges are osmotically stressed, but also when an external, nonosmotic force is applied (sarcomere stretching). Furthermore, our model predicts (see Results), that lowering cross-bridge deformation by applying an external, nonosmotic force at constant protein osmotic pressure decreases the water activity coefficient. This indicates that new water-myosin interactions are formed or preexisting water-myosin interactions are strengthened, or both. Melting of the water structure is, on the contrary, expected when an external, nonosmotic force increases the elastic deformation of the cross-bridges. We predict that similar events occur in muscle in the course of the power stroke and that the power stroke is accompanied both by a significant rearrangement of the structure of water and by osmotic phenomena.

### The osmotic behavior of skeletal muscle

In the recent past the effect of small and large osmolytes on the behavior of skeletal muscle was extensively investigated (Sato, 1954; Blinks, 1965; Rome, 1968; Millman et al., 1981; Gulati and Babu, 1982; Millman and Irving, 1988; Irving and Millman, 1992). In our opinion, however, insufficient attention was paid to the fact that contractile activity per se is the cause of osmotic changes. Although the volume of muscle filament lattice is reported to be approximately constant, the filament lattice spacing changes with the length of the sarcomere. Thus, both passive stretching and active shortening of the sarcomere are potential causes of significant osmotic changes, as we have shown in our studies on the formation of actomyosin (Magri et al., 1996). The change from normal Ringers to hyperosmotic solutions produces a comparatively smaller decrease of the 1.0 lattice

spacing in muscles stretched beyond filament overlap (3.6–4.3  $\mu\text{m}$ ) than in muscle at shorter sarcomere length (Millman et al., 1981). This also indicates a different osmotic regime of the sarcomere as a function of stretching. Power stroke itself, because of cross-bridge deformation, may originate rapid pulses of water-chemical potential changes.

Unfortunately, proper definition of the osmotic phenomena in vivo requires a detailed knowledge of the constraints on the contractile apparatus and of the direction and time scale of the water fluxes during contraction. There is an upper limit of  $\sim 40$  nm to swelling of intact frog sartorius muscle in hypotonic solutions (Rome, 1968; Irving et al., 1992). This limit is similar to that found in skinned frog sartorius muscle, suggesting that the same constraints are operating in the two cases (Millman and Irving, 1988). Furthermore, comparison of the data of Irving and Millman (1992) on the A-band lattice of intact skeletal muscle with measurements of fiber width using light microscopy (Gulati and Babu, 1982) indicate a similar behavior between lattice and fiber swelling when osmolarity is varied within 20% of normal values (0.19–0.29 Osm). Beyond these limits, changes in fiber width are greater than changes in lattice spacing. The difference, however, could be traced to the fact that fibers in muscle, because of the mutual compression, experience a larger constraint than intact single fibers.

Information on water fluxes is important to understand whether sarcomere sliding occurs at constant volume (in this case a change of the water chemical potential is expected) or the volume changes (in this case a change of the water activity coefficient is expected). Even though the volume of muscle filament lattice is reported to be constant, we must consider that even a volume change of  $\sim 1\%$  would induce significant osmotic changes. Information on the rate of water fluxes is also required. To keep up in adjusting the osmotic equilibria these rates should be larger than the rate of sarcomere shortening.

Proper modeling of the energy partition during the power stroke thus requires careful consideration of the osmotic factors in addition to the chemoelastic ones.

This work was supported by grants from the University of Ferrara, the Italian Ministero dell'Università e della Ricerca Scientifica, and by Grant 98.00464.CT04 of the Italian CNR.

### REFERENCES

- Blinks, J. R. 1965. Influence of osmotic strength on cross-section and volume of isolated single muscle fibres. *J. Physiol. (Lond.)* 177:42–57.
- Brokaw, C. J. 1976. Computer simulation of movement-generating cross-bridges. *Biophys. J.* 16:1013–1027.
- Craig, R., and G. Hoffer. 1976. Axial arrangement of crossbridge in tick filaments of vertebrate skeletal muscle. *J. Mol. Biol.* 102:325–332.
- Grazi, E. 1997. Hypothesis. What is the diameter of the actin filament? *FEBS Lett.* 405:249–252.

- Grazi, E., E. Magri, C. Schwenbacher, and G. Trombetta. 1994. Actin may contribute to the power stroke in the binary actomyosin system. *Biochem. Biophys. Res. Commun.* 200:59–64.
- Grazi, E., E. Magri, C. Schwenbacher, and G. Trombetta. 1995. Osmotic properties of myosin subfragment 1: implications on the mechanism of muscle contraction. *Arch. Biochem. Biophys.* 322:97–102.
- Grazi, E., E. Magri, C. Schwenbacher, and G. Trombetta. 1996a. Hypothesis. The stiffness of the crossbridge is a function of the intrinsic protein osmotic pressure generated by the crossbridge itself. *FEBS Lett.* 387: 101–104.
- Grazi, E., E. Magri, C. Schwenbacher, and G. Trombetta. 1996b. A model relating protein osmotic pressure to the stiffness of the cross-bridge components and the contractile force of skeletal muscle. *Eur. J. Biochem.* 241:25–31.
- Grazi, E., C. Schwenbacher, and E. Magri, 1993. Osmotic stress is the main determinant of the diameter of the actin filament. *Biochem. Biophys. Res. Commun.* 197:1377–1381.
- Gulati, J., and A. Babu. 1982. Tonicity effects on intact single muscle fibres: relation between force and cell volume. *Science.* 215:1109–1112.
- Honda, H., and S. Asakura. 1989. Calcium-triggered movement of regulated actin in vitro. A fluorescence microscopy study. *J. Mol. Biol.* 205:677–683.
- Ip, W., and J. Heuser. 1983. Direct visualization of the myosin cross-bridge helices on relaxed rabbit psoas thick filaments. *J. Mol. Biol.* 17:105–109.
- Irving, T. C., and B. M. Millman. 1992. Z-line/I-band and A-band lattices of intact frog sartorius muscle at altered intrafilament spacing. *J. Muscle Res. Cell Motil.* 13:100–105.
- Kielley, W. W., and W. F. Harrington. 1960. A model for the myosin molecule. *Biochim. Biophys. Acta.* 41:401–421.
- Magri, E., P. Cuneo, G. Trombetta, and E. Grazi. 1996. The osmotic properties and free energy of formation of the actomyosin rigor complexes from rabbit muscle. *Eur. J. Biochem.* 239:165–171.
- Margossian, S. A., and S. Lowey. 1982. Preparation of myosin and its subfragments from rabbit skeletal muscle. *Methods Enzymol.* 85:55–71.
- Millman, B. M., and T. C. Irving. 1988. Filament lattice of frog striated muscle. Radial forces, lattice stability, and filament compression in the A-band of relaxed and rigor muscle. *Biophys. J.* 54:437–447.
- Millman, B. M., T. J. Racey, and I. Matsubara. 1981. Effects of hyperosmotic solutions on the filament lattice of intact frog skeletal muscle. *Biophys. J.* 33:189–202.
- Rome, E. M. 1968. X-ray diffraction study of the filament lattice of striated muscle in various bathing media. *J. Mol. Biol.* 37:331–344.
- Sato, T. G. 1954. Osmosis of isolated single muscle fibres. *Annot. Zool. Jpn.* 27:157–164.
- Schwenbacher, C., E. Magri, G. Trombetta, and E. Grazi. 1995. Osmotic properties of the calcium-regulated actin filament. *Biochemistry.* 34: 1090–1095.
- Sjostrom, M. and J. M. Squire. 1977. Fine structure of the A-band in cryosections. The structure of the A-band of human skeletal muscle fibres from ultrathin cryosections negatively stained. *J. Mol. Biol.* 102: 49–68.